Molecular Biology of the Cell
Vol. 21, 1305–1313, April 1, 2010

The Ero1α-PDI Redox Cycle Regulates Retro-Translocation of Cholera Toxin

Paul Moore, Kaleena M. Bernardi, and Billy Tsai

Department of Cell and Developmental Biology, University of Michigan Medical School, Ann Arbor, MI 48109

Submitted September 28, 2009; Revised January 15, 2010; Accepted January 26, 2010
Monitoring Editor: Ramanujan S. Hegde

Cholera toxin (CT) is transported from the plasma membrane of host cells to the endoplasmic reticulum (ER) where the catalytic CTA1 subunit retro-translocates to the cytosol to induce toxicity. Our previous analyses demonstrated that the ER oxidoreductase protein disulfide isomerase (PDI) acts as a redox-dependent chaperone to unfold CTA1, a reaction postulated to initiate toxin retro-translocation. In its reduced state, PDI binds and unfolds CTA1; subsequent oxidation of PDI by Ero1α enables toxin release. Whether this in vitro model describes events in cells that control CTA1 retro-translocation is unknown. Here we show that down-regulation of Ero1α decreases retro-translocation of CTA1 by increasing reduced PDI and blocking efficient toxin release. Overexpression of Ero1α also attenuates CTA1 retro-translocation, an effect due to increased PDI oxidation, which prevents PDI from engaging the toxin effectively. Interestingly, Ero1α down-regulation increases interaction between PDI and Derlin-1, an ER membrane protein that is a component of the retro-translocation complex. These findings demonstrate that an appropriate Ero1α-PDI ratio is critical for regulating the binding–release cycle of CTA1 by PDI during retro-translocation, and implicate PDI's redox state in targeting it to the retro-translocon.

INTRODUCTION

Cholera toxin (CT) produced by *Vibrio cholerae* is the virulence factor responsible for the massive secretory diarrhea seen in Asiatic cholera (Sears and Kaper, 1996). Structurally, the CT holotoxin consists of a receptor-binding homopentameric B subunit (CTB) that is noncovalently associated with a single catalytic A subunit (CTA; Spangler, 1992). On secretion from *V. cholerae*, CTA is proteolytically nicked into the toxic A1 (CTA1) and the A2 (CTA2) domains, which are linked by a disulfide bond and noncovalent interactions. To intoxicate cells, CTB binds to the ganglioside receptor GM1 on the plasma membrane of intestinal epithelial cells and carries CTA from the cell surface to the lumen of the endoplasmic reticulum (ER; Fujinaga *et al.*, 2003). In this compartment, CTA is reduced, thereby generating the CTA1 peptide. It then disguises itself as a misfolded protein and engages the host cell machinery that normally retro-translocates misfolded proteins across the ER membrane to the cytosol for ubiquitin-dependent proteasomal degradation in a process called ER-associated degradation (ERAD; Hazes and Read, 1997; Tsai *et al.*, 2002; Vembar and Brodsky, 2008). On reaching the cytosol, however, the toxin escapes proteolytic destruction and induces the production of cAMP, which in turn leads to a signaling cascade that results in the opening of a chloride channel (Lencer and Tsai, 2003). The ensuing secretion of chloride ions and water across the plasma membrane results in the massive diarrhea symptomatic of cholera. How CTA1 reaches the cytosol from the ER is not fully understood.

Using an in vitro approach, we initially identified the ER-resident oxidoreductase protein disulfide isomerase (PDI) as an ER-resident protein that unfolds the CTA1 peptide (Tsai *et al.*, 2001). This unfolding event initiates toxin retro-translocation across the ER membrane. Detailed analysis showed that PDI acts as a redox-dependent chaperone in the unfolding reaction (Tsai *et al.*, 2001). In its reduced state, PDI binds and unfolds CTA1, whereas subsequent oxidation of PDI by Ero1α, an established PDI oxidase (Frand and Kaiser, 1998; Pollard *et al.*, 1998; Cabibbo *et al.*, 2000; Sevier and Kaiser, 2008), promotes toxin release (Tsai and Rapoport, 2002). Thus, reduced PDI has a higher affinity for CTA1, whereas oxidized PDI displays a lower affinity for the toxin. Although we have since demonstrated that PDI is crucial for retro-translocation of CTA1 in cells (Forster *et al.*, 2006), the role of Ero1α in regulating CTA1 retro-translocation remains unknown.

In addition, as unfolded CTA1 refolds rapidly once it is released from PDI (Rodighiero *et al.*, 2002), we hypothesized that the Ero1α-PDI complex must be coupled physically to the retro-translocation machinery on the ER membrane such that the released toxin can cross the retro-translocon without refolding. Although we found previously that Derlin-1, an ER membrane protein that is a component of the retro-translocon (Lilley and Ploegh, 2004; Ye *et al.*, 2004), binds to PDI and facilitates CTA1 retro-translocation (Bernardi *et al.*, 2008), the precise mechanism by which PDI engages Derlin-1 is not clear.

In this study, we used loss-of-function and gain-of-function approaches to assess the role of Ero1α in facilitating retro-translocation of CTA1. We found that down-regulation of Ero1α attenuates retro-translocation of CTA1 by increasing reduced PDI levels and blocking toxin release. Similarly,

This article was published online ahead of print in *MBoC in Press* (http://www.molbiolcell.org/cgi/doi/10.1091/mbc.E09–09–0826) on February 3, 2010.

Address correspondence to: Billy Tsai (btsai@umich.edu).

Abbreviations used: CT, cholera toxin; PDI, protein disulfide isomerase; ER, endoplasmic reticulum; ERAD, ER-associated degradation; TCRα, T-cell receptor alpha.

overexpression of Ero1α decreases CTA1 retro-translocation by increasing oxidation of PDI, thus preventing it from engaging the toxin efficiently. Intriguingly, we show that Ero1α down-regulation increases the interaction between PDI and Derlin-1. These findings demonstrate that Ero1α plays a crucial function in mediating CTA1 retro-translocation at two distinct steps. First, Ero1α controls the binding-release cycle of CTA1 from PDI during retro-translocation, and second, regulates the association of PDI with a component of the retro-translocon.

MATERIALS AND METHODS

Materials

Primary antibodies used were as follows: polyclonal PDI, polyclonal Hsp90 (Santa Cruz Biotechnology, Santa Cruz, CA), monoclonal PDI, polyclonal CTB (Abcam, Cambridge, MA), polyclonal Ero1α (Cell Signaling Technology, Beverly, MA), monoclonal BiP (BD Biosciences, San Jose, CA), monoclonal FLAG (Sigma-Aldrich, St. Louis, MO), and monoclonal p97 (RDI Division of Fitzgerald Industries International, Concord, MA). Monoclonal antibodies against Myc and HA were gifts from K. Verhey (University of Michigan, Ann Arbor, MI). The polyclonal antibody against Derlin-1 was a gift from T. Rapoport (Harvard Medical School, Boston, MA). The polyclonal antibody against ERp57 was a gift from S. High (University of Manchester, Manchester, England). The polyclonal CTA antibody was produced against denatured CTA purchased from EMD Biosciences (San Diego, CA). Purified CT was purchased from EMD Biosciences. HA-tagged CD3δ and T-cell receptor alpha (TCRα) expression plasmids were gifts from C. Wojcik (Indiana University, Indianapolis, IN).

Mutagenesis of Ero1α

Mutagenesis of Ero1α was achieved using the Stratagene QuikChange II Site-directed Mutagenesis Kit (La Jolla, CA) and a pcDNA3.1(+)-Ero1α plasmid construct (a gift from Roberto Sitia (Università Vita-Salute–San Raffaele Scientific Institute) as a template for generation of the Cys94 to Ala94 mutant. The resulting pcDNA3.1(+)-C94A Ero1α construct was used in turn as a template for the generation of the pcDNA3.1(+)-C94A:C99A Ero1α construct. The mutated Ero1α constructs were confirmed by sequencing.

Tissue Culture, Transfection, and Protein Down-Regulation

HEK293T cells were cultured in DMEM with 10% fetal bovine serum (FBS) and penicillin/streptomycin. All expression constructs used were transfected into 30% confluent cells on 10- or 6-cm dishes using the Effectene system (Qiagen, Chatsworth, CA). Small interfering RNA (siRNA) against Ero1α (5′-UUUCUAACCAGGUCUCUUGUU-3′) was synthesized by Invitrogen (Carlsbad, CA). Duplexed siRNA at 200 nM was transfected into 15–30% confluent 293T cells using Oligofectamine (Invitrogen) according to the manufacturer's protocol.

XBP1 Splicing

Splicing was as described previously in Uemura *et al.* (2009).

Retro-Translocation Assay

293T cells were intoxicated with 10 nM CT in HBSS for 45 min at 37°C. Cells (2×10^6) were permeabilized in 100 μl of 0.01% digitonin in HCN buffer (50 mM HEPES, pH 7.5, 150 mM NaCl, 2 mM $CaCl_2$, 10 mM *N*-ethylmaleimide [NEM], and protease inhibitors), incubated on ice for 10 min, and centrifuged at 16,000 × *g* for 10 min at 4°C. The supernatant was removed, and the pellet was resuspended in 100 μl of sample buffer. Fractions were analyzed by nonreducing SDS-PAGE and immunoblot.

cAMP Assay

CT-induced cAMP levels were analyzed as previously described (Forster *et al.*, 2006).

Pulse-Chase Analysis of TCRα

Analysis of TCRα-hemagglutinin (HA) degradation followed a previously published protocol (Zhang *et al.*, 2002).

Mal-PEG Modification

In vivo analysis of PDI and ERp57 reduction/oxidation states was done using the double NEM-alkylation variant of mal-PEG (maleimide polyethylene glycol 5000) modification that was previously described (Appenzeller-Herzog and Ellgaard, 2008). The protocol was modified to exclude metabolic labeling. Instead, samples were analyzed by nonreducing SDS-PAGE and immunoblot.

Immunoprecipitation and Chemical Cross-Linking

293T cells were incubated with or without 100 nM CT for 90 min as indicated. Where indicated, NEM (5 mM) was added to the cells for 30 min after the cells were initially exposed to CT for 60 min. Cells were then harvested, lysed in a buffer containing Tris-HCl (30 mM), pH 7.5, $MgCl_2$ (4 mM), KOAc (150 mM), and NEM (10 mM) with either 1% deoxy BigChap (DBP) or 1% Triton X-100, and centrifuged for 10 min at 16,000 × *g*. The supernatant was collected and used for immunoprecipitation. The specified antibodies were added to the supernatant and incubated overnight at 4°C. Immune complexes were captured by addition of protein A agarose beads (Invitrogen), washed, and subjected to nonreducing SDS-PAGE and immunoblot analysis. Where designated, cells were subjected to in vivo cross-linking by incubation with 2 mM dithiobis succinimidyl propionate (DSP; Thermo Fisher Scientific, Waltham, MA) in PBS for 30 min before lysis. All cross-linked samples were reduced by boiling for 5 min in sample buffer containing 5% β-mercaptoethanol before analysis.

RESULTS

Ero1α Down-Regulation Decreases Retro-Translocation of CTA1

We down-regulated Ero1α in 293T cells to assess its requirement in retro-translocation of CTA1. Cells were treated with either a control (scrambled) or an Ero1α-specific siRNA and lysed, and the resulting whole cell lysates (WCL) were subjected to nonreducing SDS-PAGE and immunoblotted with the indicated antibodies. We found that the Ero1α protein level in cells treated with the Ero1α-specific siRNA (Ero1α$^-$ cells) was reduced significantly when compared with control cells (Figure 1A, top panel, cf. lane 2 with lane 1). Under this condition, the unfolded protein response (UPR) markers BiP, PDI, and Derlin-1 (Oda *et al.*, 2006) were not up-regulated to any significant extent (Figure 1A, second, third, and fourth panels, cf. lane 2 with lane 1). Expression of Ero1β, the other Ero1 isoform, was also not affected (Figure 1A, fifth panel, cf. lane 2 with lane 1). Furthermore, neither transfection of the scrambled nor Ero1α-specific siRNA triggered the splicing of the XBP1 transcription factor mRNA, in contrast to incubating cells with the known ER stress inducers dithiothreitol (DTT) and tunicamycin (Figure 1A, cf. lanes 3 and 4 with lanes 5 and 6). These findings indicate that down-regulation of Ero1α does not trigger massive ER stress.

To measure toxin retro-translocation, control and Ero1α$^-$ cells were subjected to a previously established ER-to-cytosol retro-translocation assay (Forster *et al.*, 2006; Bernardi *et al.*, 2008). In this assay, cells were intoxicated with 10 nM CT for 45 min, harvested, and treated with a low digitonin concentration (0.01%) to permeabilize the plasma membrane while leaving intracellular membranes intact. Cells were then subjected to fractionation by centrifugation to separate cytosolic (supernatant) and membrane (pellet) fractions. As expected, the cytosolic Hsp90 protein is present in the supernatant fraction (Figure 1B, fourth panel). The majority of PDI, an ER lumenal protein, was present in the pellet but not in the supernatant fraction (Figure 1B, cf. seventh and third panels), demonstrating that the ER membrane was not disrupted significantly by digitonin treatment. Thus, any CTA1 that appears in the supernatant is not due to nonspecific leakage but instead represents retro-translocated toxin. Several control experiments validated this assay. First, we found previously that CTA1 does not appear in the supernatant in cells treated with brefeldin A (an agent that blocks COPI-dependent retrograde transport to the ER), nor in cells incubated at 4°C (a condition that blocks endocytosis; Forster *et al.*, 2006; Bernardi *et al.*, 2008). Second, a mutant CT that is presumed to not undergo ER-to-cytosol transport does not appear in the supernatant (Forster *et al.*, 2006). And third, conditions that blocked CT-induced cAMP synthesis

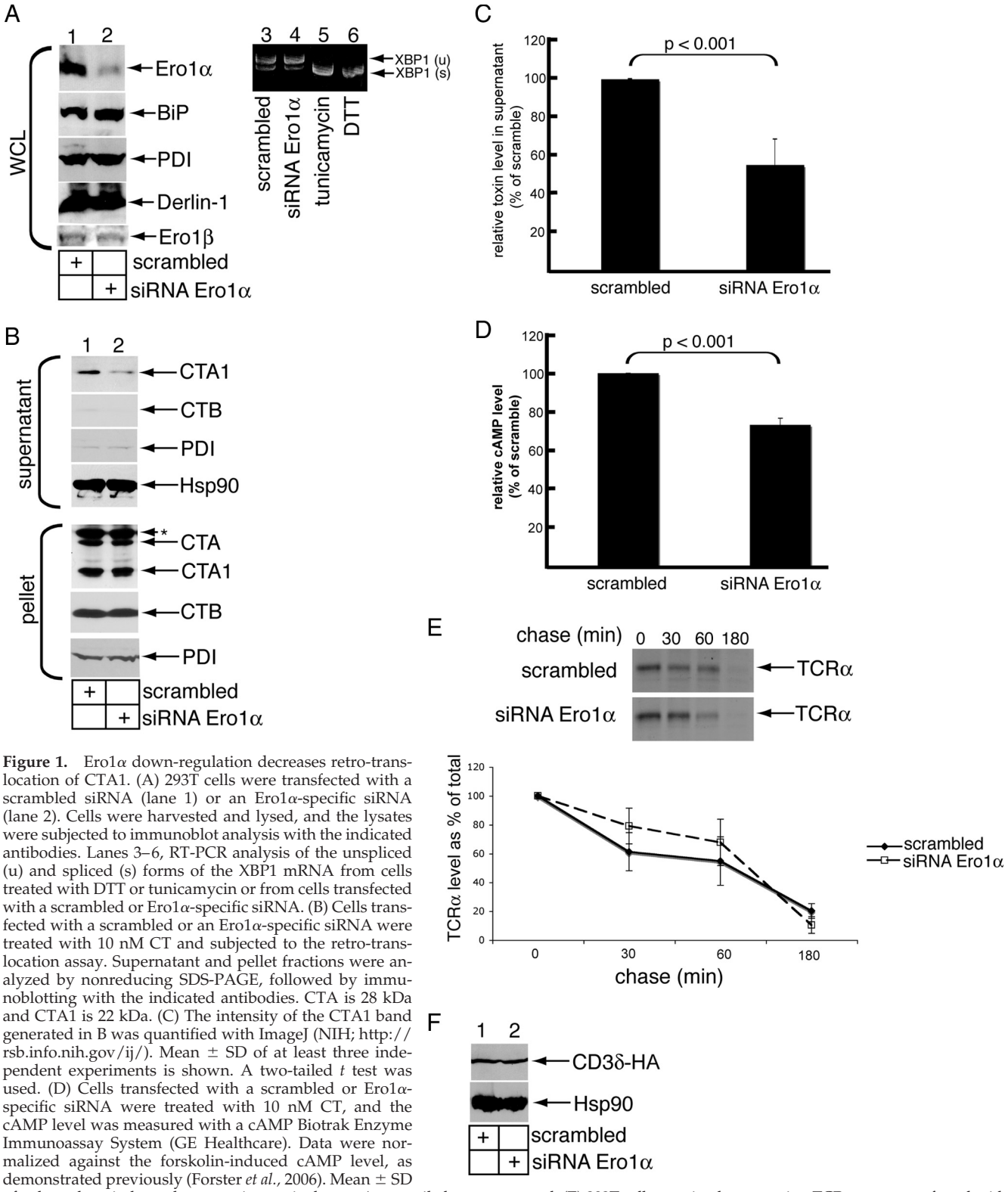

Figure 1. Ero1α down-regulation decreases retro-translocation of CTA1. (A) 293T cells were transfected with a scrambled siRNA (lane 1) or an Ero1α-specific siRNA (lane 2). Cells were harvested and lysed, and the lysates were subjected to immunoblot analysis with the indicated antibodies. Lanes 3–6, RT-PCR analysis of the unspliced (u) and spliced (s) forms of the XBP1 mRNA from cells treated with DTT or tunicamycin or from cells transfected with a scrambled or Ero1α-specific siRNA. (B) Cells transfected with a scrambled or an Ero1α-specific siRNA were treated with 10 nM CT and subjected to the retro-translocation assay. Supernatant and pellet fractions were analyzed by nonreducing SDS-PAGE, followed by immunoblotting with the indicated antibodies. CTA is 28 kDa and CTA1 is 22 kDa. (C) The intensity of the CTA1 band generated in B was quantified with ImageJ (NIH; http://rsb.info.nih.gov/ij/). Mean ± SD of at least three independent experiments is shown. A two-tailed *t* test was used. (D) Cells transfected with a scrambled or Ero1α-specific siRNA were treated with 10 nM CT, and the cAMP level was measured with a cAMP Biotrak Enzyme Immunoassay System (GE Healthcare). Data were normalized against the forskolin-induced cAMP level, as demonstrated previously (Forster *et al.*, 2006). Mean ± SD of at least three independent experiments is shown. A two-tailed *t* test was used. (E) 293T cells transiently expressing TCRα were transfected with a scrambled or an Ero1α-specific siRNA, labeled with [^{35}S]methionine, and harvested at the indicated chase times, and the resulting cell lysate was used for TCRα immunoprecipitation. Signals were detected by autoradiography. Bottom panel, quantification of the intensity of the TCRα band from three independent experiments; values are expressed as a total percentage of the TCRα band at chase time = 0. Error bars, ±SD.

also caused a decrease in CTA1 level in the supernatant (Forster *et al.*, 2006; Bernardi *et al.*, 2008).

Using this assay, we found that the level of CTA1 in the supernatant of Ero1α$^-$ cells is decreased when compared

with control cells (Figure 1B, top panel, cf. lane 2 with lane 1; quantified in Figure 1C). Likewise, we also measured the CT-induced cAMP level in control and Ero1α^- cells and found that the cAMP level decreased in the Ero1α^- cells when compared with control cells (Figure 1D). Together, these findings indicate that Ero1α plays an important role in regulating CTA1 retro-translocation.

We then asked if down-regulation of Ero1α affects the degradation of other retro-translocation substrates, including TCRα (Yu *et al.*, 1997) and CD3δ (Tiwari and Weissman, 2001). Metabolic pulse-chase experiments showed that the rate of TCRα degradation was not significantly disrupted in Ero1α^- cells when compared with control cells (Figure 1E, top two panels; quantified below). Similarly, the steady-state level of transfected HA-tagged CD3δ was the same in control and Ero1α^- cells (Figure 1F, top panel, cf. lanes 1 and 2). These data demonstrate that Ero1α does not play a critical function in the retro-translocation of two established retro-translocation substrates, but instead facilitates CTA1 retro-translocation specifically.

Ero1α Overexpression Attenuates Retro-Translocation of CTA1

In conjunction with this loss-of-function approach, we used a gain-of-function strategy to test the role of Ero1α in mediating toxin retro-translocation. To this end, wild-type (WT) Ero1α was overexpressed in 293T cells (Figure 2A, top panel, cf. lane 2 with lane 1). We also overexpressed an enzymatically inactive form of Ero1α (Bertoli *et al.*, 2004) in which the catalytic cysteines at positions 94 and 99 were mutated to alanine [i.e., Ero1α(C94A:C99A)] to the same extent as WT Ero1α (Figure 2A, top panel, cf. lane 4 with lane 3). To assess potential cellular stress caused by overexpressing WT Ero1α, we found that overexpression of WT Ero1α affects neither the levels of PDI, BiP, and Derlin-1 (Figure 2A, second, third, and fourth panels, cf. lane 2 with lane 1) nor splicing of XBP1 (Figure 2A, cf. lanes 5 and 6 with lanes 7 and 8). These findings indicate that overexpressing Ero1α does not profoundly trigger ER stress.

To determine whether this gain-of-function approach affects toxin retro-translocation, cells overexpressing WT Ero1α and Ero1α(C94A:C99A), as well as vector-transfected cells, were subjected to the retro-translocation assay as described in Figure 1. We found that in cells overexpressing WT Ero1α, but not Ero1α(C94A:C99A), the level of CTA1 in the supernatant decreased when compared with vector-transfected cells (Figure 2B, top panel, cf. lane 2 with lanes 1 and 3; quantified in Figure 2E). CTA1 retro-translocation also decreased in cells overexpressing dominant-negative Derlin-1 (i.e., Derlin-1-YFP; quantified in Figure 2E), consistent with our previous finding (Bernardi *et al.*, 2008). These data indicate that increasing the level of the enzymatic-active Ero1α perturbs retro-translocation of CTA1.

Because down-regulation (Figure 1) and overexpression of Ero1α (Figure 2) both resulted in decreased CTA1 retro-translocation, we reasoned that a proper steady-state ratio of Ero1α to PDI in cells might be important for driving toxin retro-translocation. Thus, in cells overexpressing WT Ero1α (Figure 2C, lane 2), we tested whether or not overexpressing PDI simultaneously with WT Ero1α (Figure 2C, lane 3) to restore the appropriate Ero1α-PDI ratio would functionally restore retro-translocation of the toxin, and found that it did (Figure 2D, top panel, cf. lane 3 with lane 2; quantified in Figure 2E). These findings not only demonstrate a functional role of Ero1α in ejecting CTA1 into the cytosol, but further suggest that a proper Ero1α-PDI ratio is critical for this process. Interestingly, overexpression of Ero1β did not appear to affect toxin retro-translocation (Figure 2E).

Altering the Ero1α Level in Cells Affects the Redox State of PDI

The ability of catalytically active Ero1α to regulate CTA1 retro-translocation in a PDI-specific manner suggests that Ero1α controls PDI–substrate interaction in a redox-dependent manner. PDI contains six cysteines: two in the so called redox-active thioredoxin *a* domain, two in the redox-active thioredoxin *a*′ domain, and two additional cysteines in redox-inactive domains. The cysteines in the redox-active *a* and *a*′ domains cycle between the oxidized and reduced states. To test if down-regulation or overexpression of WT Ero1α changes the PDI redox state, we took advantage of an approach that measures the in vivo redox state of PDI (Appenzeller-Herzog and Ellgaard, 2008). Briefly, cells were incubated with the alkylating agent NEM to modify free cysteines on PDI and lysed, and the PDI was immunoprecipitated from the resulting lysate. Any disulfide-bonded cysteines in PDI were subsequently reduced by the strong reducing agent tris(2-carboxyethyl) phosphine (TCEP), followed by washing to remove excess TCEP. The newly formed free cysteines were then modified by the 5-kDa thiol-modifying reagent maleimide PEG 5000 (MPEG), and the immunoprecipitated sample was subjected to SDS-PAGE followed by immunoblotting with a PDI-specific antibody. Higher molecular weight PDI species represent MPEG-modified PDI. It is important to note that in this approach only cysteines in PDI that are originally in the oxidized, but not reduced, state are modified by MPEG.

In the presence of MPEG, the various redox forms of PDI in cells at steady state could indeed be detected (Figure 3A, cf. lane 2 with lane 1); the designation of specific redox forms of PDI corresponding to particular bands on the immunoblot is based on previous analysis (Appenzeller-Herzog and Ellgaard, 2008). Importantly, the pool of high-molecular-weight PDI species in the Ero1α^- cells was less when compared with PDI in control cells (Figure 3B, cf. lane 2 with lane 1), indicating less modification of PDI in the Ero1α^- cells. In contrast, using this same method, we found that the redox state of ERp57 was not affected in the Ero1α^- cells when compared with control cells (Figure 3C, cf. lane 2 with lane 1); this result is consistent with a previous finding that showed that Ero1α does not control the redox state of ERp57 (Mezghrani *et al.*, 2001). These findings demonstrate that PDI, but not ERp57, is oxidized less in Ero1α^- cells, thereby confirming that Ero1α functions as a PDI oxidase. Thus, the block of CTA1 retro-translocation observed in the Ero1α^- cells (Figure 1) can be attributed to a decrease in the pool of oxidized PDI.

Conversely, when Ero1α was overexpressed, we found that the pool of high-molecular-weight PDI species increased when compared with PDI in vector-transfected cells (Figure 3D, cf. lane 2 with lane 1), thereby indicating that PDI is oxidized more in Ero1α-overexpressing cells. Hence, the decrease in toxin retro-translocation observed in Ero1α-overexpressing cells (Figure 2) is likely due to an increase in the pool of oxidized PDI.

The Level of Ero1α Controls PDI–CTA1 Interaction

According to the redox-dependent model, reduced PDI binds and unfolds CTA1 (Tsai *et al.*, 2001); subsequent oxidation of PDI by Ero1α releases the toxin (Tsai and Rapoport, 2002). As such, this model would suggest that a lack of Ero1α would preclude PDI oxidation, effectively trapping the toxin on PDI. We have shown thus far that a decrease in the level of Ero1α decreases both the pool of oxidized PDI and CTA1 retro-translocation. Mechanistically, the simplest explanation of these results is that CTA1 is released inefficiently

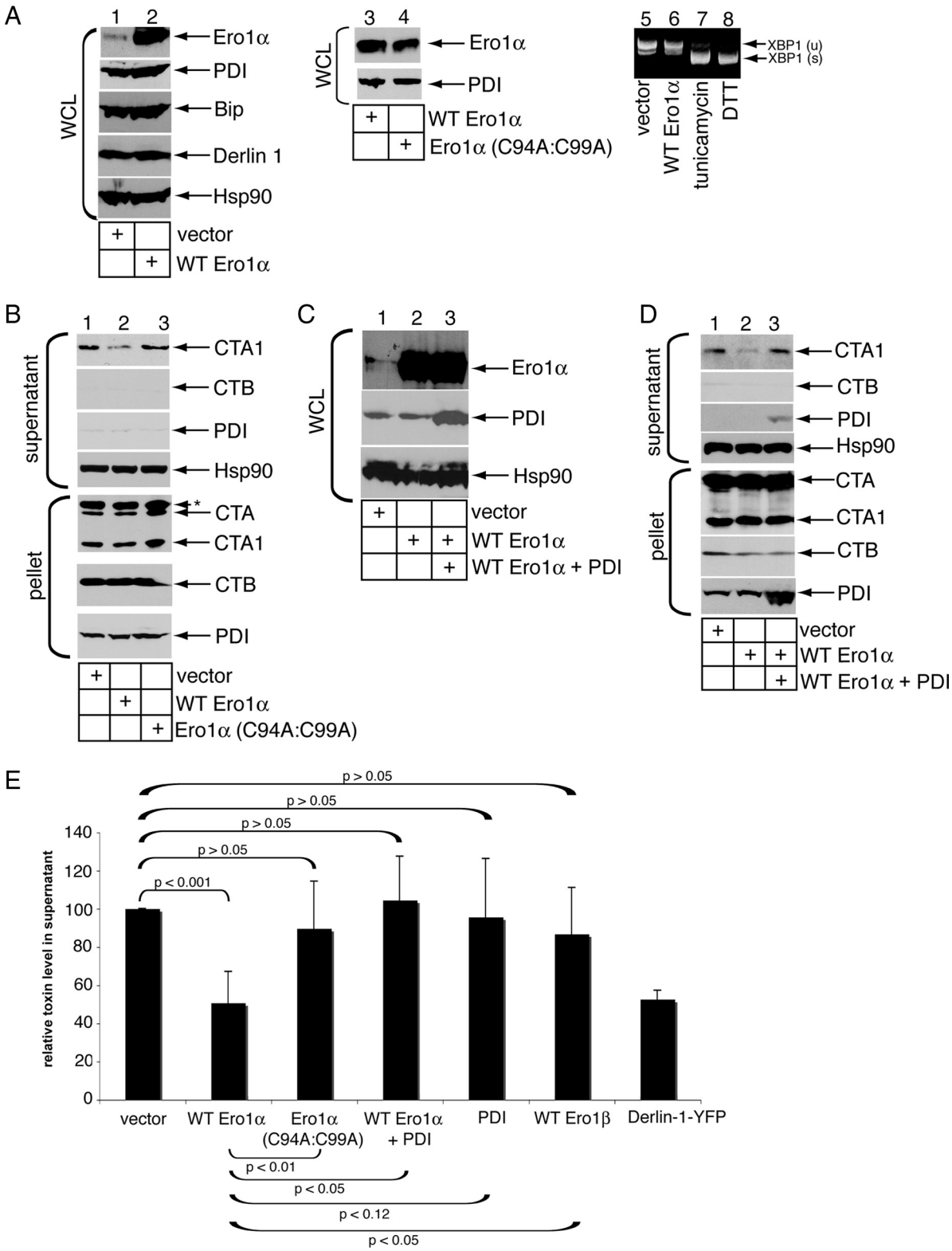

Figure 2. Ero1α overexpression attenuates retro-translocation of CTA1. (A) Lanes 1–4, lysates from 293T cells transfected with vector, WT Ero1α, or Ero1α(C94A:C99A) were analyzed for expression of Ero1α, BiP, PDI, Derlin-1, and Hsp90. Lanes 5–8, RT-PCR analysis of the unspliced (u) and spliced (s) forms of the XBP1 mRNA from cells treated with DTT or tunicamycin or from cells transfected with vector or a WT Ero1α construct. (B) Cells in A were subjected to the retro-translocation assay as described in Figure 1. (C) Lysates from 293T cells transfected with vector, WT Ero1α, or WT Ero1α and PDI were analyzed for expression of Ero1α, PDI, and Hsp90. (D) Cells in C were subjected to the retro-translocation assay as in Figure 1. (E) Quantification of the CTA1 band intensity in B and D. Mean ± SD of at least three independent experiments is shown. A two-tailed *t* test was used. Results from overexpression of Ero1β and Derlin-1-YFP on CTA1 retro-translocation are also included.

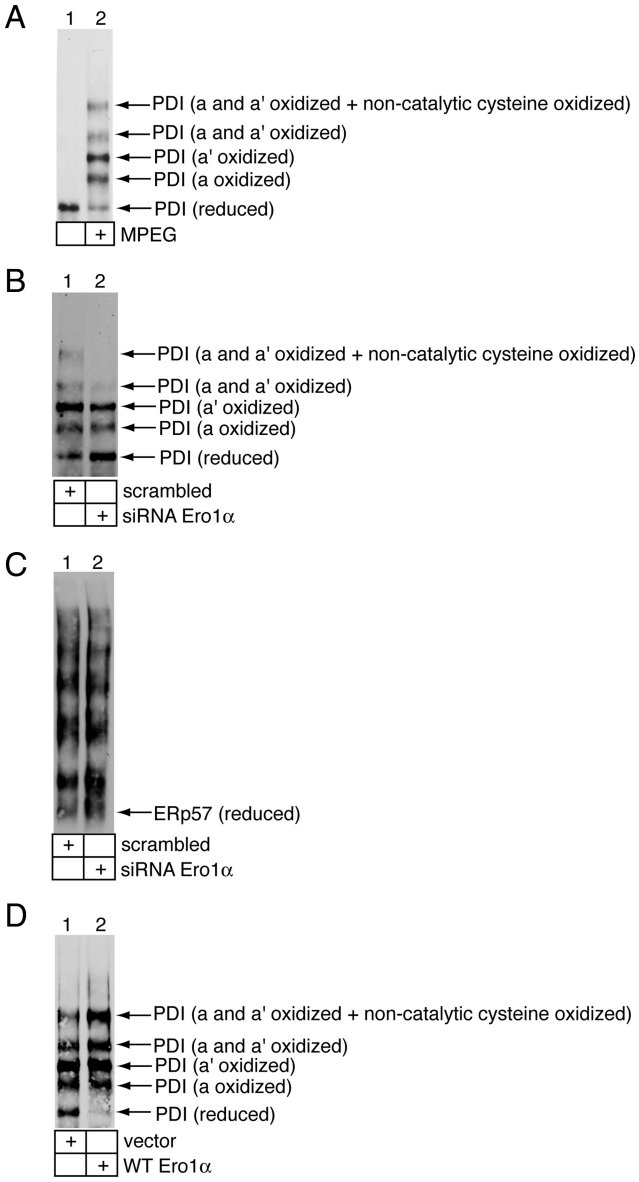

Figure 3. Altering Ero1α level in cells affects the redox state of PDI. (A) 293T cells were treated with NEM and lysed, and the endogenous PDI was immunoprecipitated from the lysate. The immunoprecipitate was incubated with TCEP, washed, and treated with or without MPEG. Samples were analyzed by SDS-PAGE and immunoblotted with an antibody against PDI. (B) 293T cells transfected with a scrambled or an Ero1α-specific siRNA were analyzed as in A, with the exception that both samples were treated with MPEG. (C) As in B, except ERp57 was immunoprecipitated and immunoblotted instead of PDI. (D) 293T cells transfected with vector or WT Ero1α were analyzed as in B.

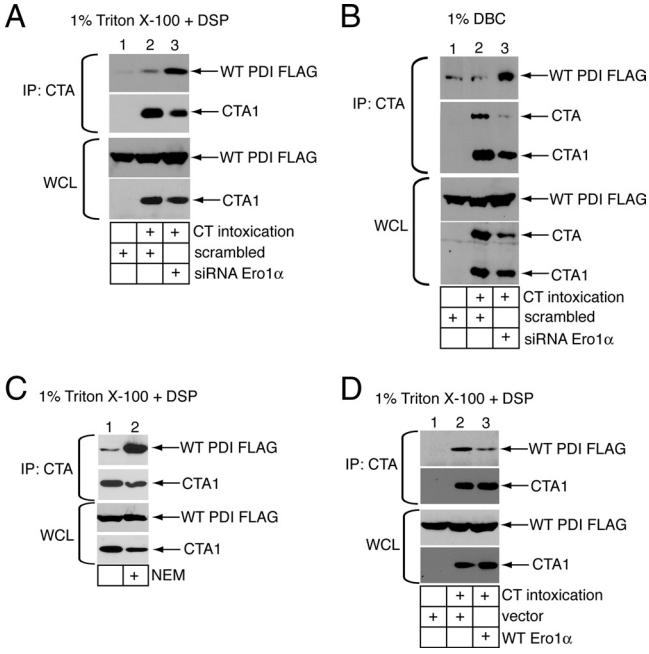

Figure 4. The level of Ero1α controls PDI–CTA1 interaction. (A) 293T cells were transfected with WT PDI FLAG and either a scrambled or an Ero1α-specific siRNA, followed by incubation of the cells with or without CT. DSP cross-linker was added to the cells, followed by lysis with 1% Triton X-100. A CTA-specific antibody was incubated with the resulting lysate, and the precipitated sample was subjected to reducing SDS-PAGE followed by immunoblotting with the indicated antibodies. (B) As in A, except no DSP was added, and DBC was used instead of Triton X-100. Samples were subjected to nonreducing SDS-PAGE. (C) Cells overexpressing WT PDI FLAG were treated with or without NEM 60 min after CT intoxication, and the PDI–CTA1 interaction was analyzed as in A. (D) As in A, except cells were transfected with either vector or WT Ero1α.

from PDI in Ero1α$^-$ cells. To test this prediction, we assessed the PDI–CTA1 interaction in control and Ero1α$^-$ cells. 293T cells were transfected with FLAG-tagged WT PDI (WT PDI FLAG; Sigma-Aldrich), intoxicated with CT, incubated with or without the thiol-cleavable and membrane-permeable cross-linker DSP, and lysed with either 1% Triton X-100 or 1% deoxy BigChap (DBC). CTA immunoprecipitates from the WCLs were subjected to reducing SDS-PAGE (nonreducing SDS-PAGE used for DBC lysate) and subsequently immunoblotted with the indicated antibodies.

Using the DSP and 1% Triton X-100 combination, we found that a low level of WT PDI FLAG coprecipitated with CTA1 from the intoxicated but not the nonintoxicated control cells (Figure 4A, top panel, cf. lane 2 with lane 1). Importantly, the level of WT PDI FLAG that coprecipitated with CTA1 increased in the Ero1α$^-$ cells when compared with control cells (Figure 4A, top panel, cf. lane 3 with lane 2). A similar trend was observed when cells were lysed with 1% DBC (without DSP); an increased PDI–toxin interaction was observed in the Ero1α$^-$ cells when compared with control cells (Figure 4B, top panel, cf. lane 3 with lane 2). These results, which suggest that CTA1 is trapped on reduced PDI in the Ero1α$^-$ cells, are consistent with the redox-dependent model and provide a mechanistic basis by which down-regulation of Ero1α attenuates retro-translocation of CTA1.

We used an additional method to demonstrate that the reduced form of PDI has higher affinity for CTA1 in cells. To this end, cells were treated with NEM to alkylate cellular PDI, thereby "locking" it in the reduced state. We found that PDI from cells treated with NEM binds with a much higher efficiency to CTA1 than PDI from untreated cells (Figure 4C, top panel, cf. lane 2 with lane 1), suggesting that alkylated PDI displays a higher affinity for the toxin than nonalkylated PDI. This result parallels previous in vitro data showing that alkylated PDI binds to CTA1 with high affinity (Tsai *et al.*, 2001). This finding further supports our contention that binding of PDI to CTA1 operates in a redox-driven manner.

The redox-dependent model also predicts that overexpression of Ero1α would block CTA1 retro-translocation by oxidiz-

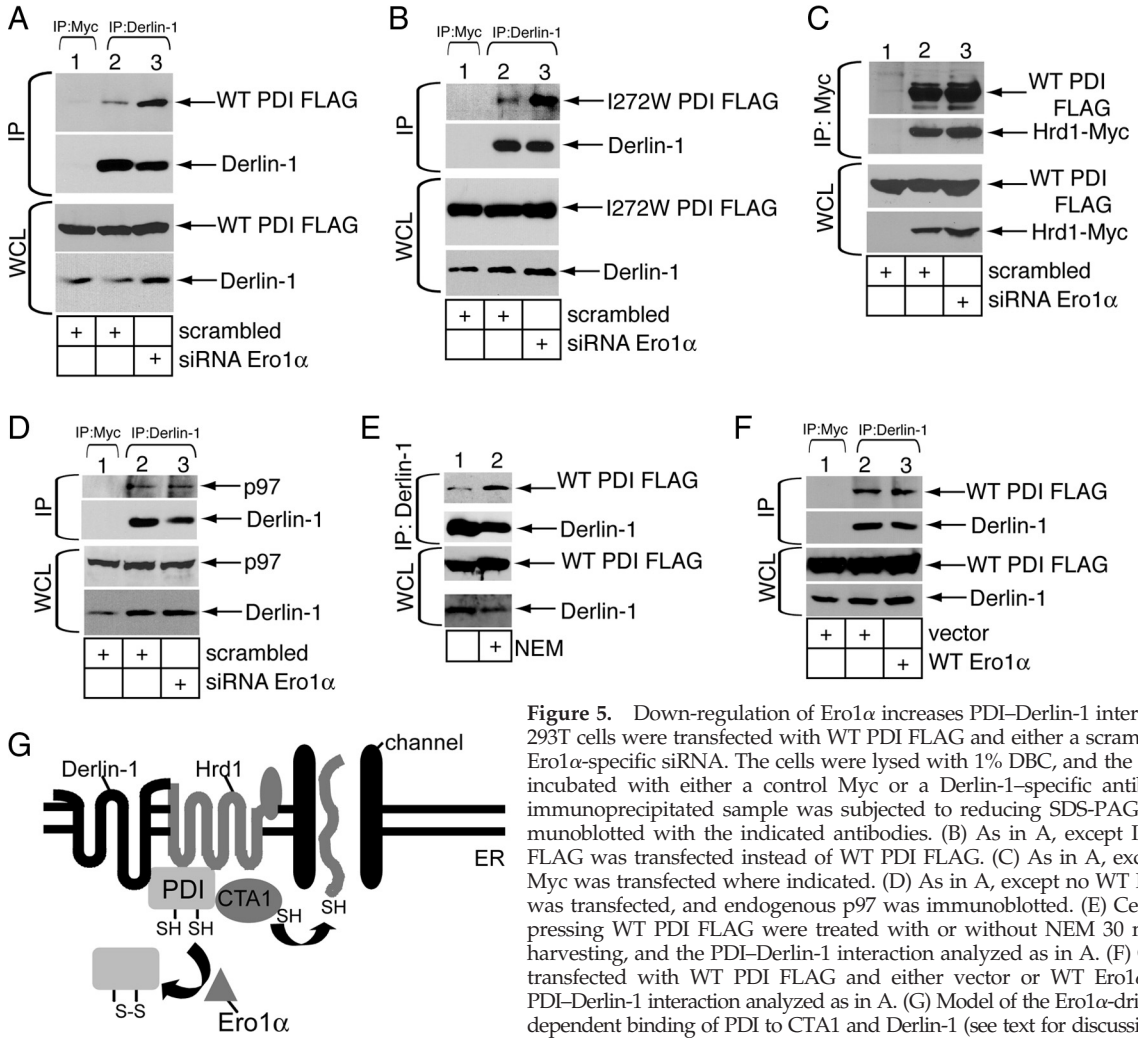

Figure 5. Down-regulation of Ero1α increases PDI–Derlin-1 interaction. (A) 293T cells were transfected with WT PDI FLAG and either a scrambled or an Ero1α-specific siRNA. The cells were lysed with 1% DBC, and the lysate was incubated with either a control Myc or a Derlin-1–specific antibody. The immunoprecipitated sample was subjected to reducing SDS-PAGE and immunoblotted with the indicated antibodies. (B) As in A, except I272W PDI FLAG was transfected instead of WT PDI FLAG. (C) As in A, except Hrd1-Myc was transfected where indicated. (D) As in A, except no WT PDI FLAG was transfected, and endogenous p97 was immunoblotted. (E) Cells overexpressing WT PDI FLAG were treated with or without NEM 30 min before harvesting, and the PDI–Derlin-1 interaction analyzed as in A. (F) Cells were transfected with WT PDI FLAG and either vector or WT Ero1α, and the PDI–Derlin-1 interaction analyzed as in A. (G) Model of the Ero1α-driven redox-dependent binding of PDI to CTA1 and Derlin-1 (see text for discussion).

ing PDI and preventing it from engaging CTA1 effectively. To test this possibility, we examined the PDI–CTA1 interaction in control and Ero1α-overexpressing cells; we found that the amount of PDI bound to toxin was in fact decreased in the Ero1α-overexpressing cells when compared with control cells (Figure 4D, top panel, cf. lane 3 with lane 2). Consequently, the decrease in CTA1 retro-translocation observed in the Ero1α-overexpressing cells (Figure 2) is likely due to the inability of oxidized PDI to engage the toxin efficiently.

Down-Regulating Ero1α Increases PDI–Derlin-1 Interaction

Our findings demonstrate that Ero1α regulates the redox state of PDI to control the binding and releasing of CTA1 in cells, steps which are essential to initiate toxin retro-translocation. However, whether the redox state of PDI affects other steps of the retro-translocation process is unknown. We found previously that PDI associates with Derlin-1 (Bernardi *et al.*, 2008), an ER membrane protein implicated as a component of the retro-translocon (Lilley and Ploegh, 2004; Ye *et al.*, 2004). This finding couples the unfolding reaction with events on the ER membrane. Here, we test if Ero1α regulation of the redox state of PDI controls the PDI–Derlin-1 interaction.

Cells were transfected with WT PDI FLAG and lysed with 1% DBC, and the lysate immunoprecipitated with a control Myc or Derlin-1-specific antibody. The immunoprecipitated samples were subjected to nonreducing SDS-PAGE and immunoblotted with the indicated antibodies. In control cells, a small amount of WT PDI FLAG was found in the Derlin-1, but not in the Myc, immunoprecipitate (Figure 5A, top panel, cf. lane 2 with lane 1), reaffirming that Derlin-1 binds to PDI (Bernardi *et al.*, 2008). Interestingly, an increased amount of PDI was found to interact with Derlin-1 in the Ero1α$^-$ cells when compared with the control cells (Figure 5A, top panel, cf. lane 3 with lane 2). This finding suggests that reduced PDI, in addition to its interaction with CTA1, exhibits a higher affinity for Derlin-1. A PDI mutant, I272W PDI, was shown previously not to interact with substrates (Pirneskoski *et al.*, 2004). We found that I272W PDI FLAG also exhibits an increased interaction with Derlin-1 in Ero1α$^-$ cells when compared with control cells (Figure 5B, top panel, cf. lane 3 with lane 2). This result indicates that Derlin-1 is an unlikely substrate of PDI; instead, it is a stable binding partner whose association with PDI is redox-regulated.

We observed recently that PDI binds to Hrd1 (Bernardi *et al.*, 2010), an integral ER membrane-bound E3 ubiquitin ligase that is a component of the retro-translocon (Ye *et al.*, 2005; Lilley and Ploegh, 2005; Schulze *et al.*, 2005). This interaction was not affected by down-regulating Ero1α (Figure 5C, top panel, cf. lane 3 with lane 2). In addition, the established interaction

between Derlin-1 and the cytosolic chaperone p97 (Ye *et al.*, 2004) was not affected by Ero1α down-regulation (Figure 5D, top panel, cf. lane 3 with lane 2). Similar to the observed increased interaction between alkylated PDI and CTA1 (Figure 4C), PDI from cells treated with NEM also interacts with Derlin-1 more efficiently than PDI from untreated cells (Figure 5E, top panel, cf. lane 2 with lane 1). Overexpression of Ero1α in cells overexpressing PDI FLAG did not alter the PDI–Derlin-1 interaction (Figure 5F, top panel, cf. lane 3 with lane 2), consistent with the functional data presented in Figure 2E. Together, the combined results from the Ero1α knockdown, overexpression and the NEM studies demonstrate that Ero1α functions to regulate the redox-dependent interaction between PDI and Derlin-1.

DISCUSSION

A decisive step in the intoxication of CT is the transfer of the toxic CTA1 subunit from the ER lumen into the cytosol. How CTA1 is prepared in the ER lumen before its arrival in the cytosol is not fully understood. Based on an in vitro approach, we determined previously that the ER lumenal proteins PDI and Ero1α likely represent two central players in this process. Specifically, we found that the reduced form of PDI binds and unfolds CTA1 (Tsai *et al.*, 2001), whereas subsequent oxidation of PDI by Ero1α releases the toxin from PDI (Tsai and Rapoport, 2002). We postulated that these events initiate retro-translocation of CTA1 in cells. Using a siRNA-mediated approach, we observed that PDI is essential for CTA1 retro-translocation (Forster *et al.*, 2006). However, the role of Ero1α in controlling the toxin retro-translocation process remained to be clarified.

Using loss-of-function and gain-of-function approaches, we have demonstrated in this study that Ero1α plays a central role in facilitating retro-translocation of CTA1. We found that down-regulation of Ero1α decreases toxin retro-translocation in a specific manner. It is not due to a general induction in ER stress as knockdown of Ero1α neither up-regulates several UPR markers, induces XBP1 splicing, nor affects the retro-translocation and degradation of the established ERAD substrates TCRα and CD3δ. Instead, we showed that down-regulation of Ero1α leads to a decrease in PDI oxidation that precludes the toxin from being released from PDI efficiently, thereby blocking toxin transport.

Likewise, overexpression of the catalytically active Ero1α also blocks CTA1 retro-translocation. In this case, increased PDI oxidation due to Ero1α overexpression prevents the toxin from engaging PDI effectively. These two findings not only pinpoint Ero1α as a critical player in toxin retro-translocation, but also support the redox-dependent model of CTA1 retro-translocation described in vitro. Furthermore, our analyses demonstrate that reduced PDI displays an increased affinity for its binding partner Derlin-1, a key component of the retro-translocon. Overall, it appears that the ability of PDI to engage a binding partner, as well as a substrate, is redox-dependent (Figure 5G). Specifically, reduced PDI engages both CTA1 and Derlin-1; oxidation of PDI by Ero1α releases the unfolded toxin from PDI as well as PDI from Derlin-1.

Our findings implicate that, under normal conditions, a cell maintains a fine balance of Ero1α and PDI levels. This balance enables sufficient amounts of reduced PDI to bind and unfold the toxin while simultaneously maintaining enough oxidation equivalents to subsequently oxidize PDI and induce toxin release. The observation that simultaneous overexpression of PDI and Ero1α rescues toxin transport further supports this idea. Although there is a much higher cellular concentration of PDI in comparison to Ero1α, only a small fraction of PDI is likely to be dedicated to retro-translocation. Consistent with this idea, we previously observed only a small fraction of PDI binds to Derlin-1 (Bernardi *et al.*, 2008); this pool of PDI is expected to be involved in retro-translocation.

The Ero1α-PDI redox cycle described in this study is not designed primarily for pathogen entry. Instead, this system is likely geared to drive the retro-translocation of misfolded substrates during ERAD (Vembar and Brodsky, 2008). For example, PDI displays redox-dependent binding to the ERAD substrates such as BACE (Molinari *et al.*, 2002) and the nonglycosylated pro-α factor (Wahlman *et al.*, 2007), suggesting Ero1α may act in the retro-translocation of these substrates. Moreover, although the specific ER factors have not yet been identified, the cellular redox state appears to control the degradation of several ER proteins (Young *et al.*, 1993; Wainwright and Field, 1997; Courageot *et al.*, 1999), signifying that the Ero1α-PDI complex may be generally involved. In addition to our finding that PDI acts as a chaperone to unfold CTA1 and initiate toxin retro-translocation, it is important to note that PDI is recognized classically as an enzyme that catalyzes the formation, breakage, and rearrangement of disulfide bonds during the protein folding process (Ellgaard and Ruddock, 2005).

We note that down-regulation of Ero1α does not block toxin retro-translocation completely. This result may be due to the incomplete knockdown of Ero1α or to the complementary activity of other undiscovered PDI oxidases. In this context, there is another isoform of Ero1 called Ero1β (Pagani *et al.*, 2000). However, our previous in vitro analysis suggested that Ero1β does not oxidize PDI to release CTA1 (Tsai and Rapoport, 2002). This result is supported by our finding that overexpression of Ero1β does not affect toxin retro-translocation (data not shown). Furthermore, Ero1β is found to be expressed at low levels in 293T cells (Pagani *et al.*, 2000), implying that Ero1β does not contribute significantly to the toxin transport process.

Structurally, the observation that PDI engages a substrate and a binding partner in a redox-dependent manner suggests that the PDI redox state may regulate the conformation of multiple binding sites. In this context, we have demonstrated previously that reduced and oxidized PDI exist in different conformations (Tsai *et al.*, 2001). Pinpointing the specific sites on PDI that bind to CTA1 (Forster *et al.*, 2009) and Derlin-1 will be crucial in assessing whether these binding sites are altered in response to the redox state of PDI.

The fact that reduced PDI binds to Derlin-1 with increased affinity has major implications for the mechanism by which the unfolding process is coupled to events on the ER membrane. Preferential targeting of reduced PDI to the retro-translocation machinery permits efficient temporal and spatial interactions with CTA1. Subsequent oxidation of PDI by Ero1α, which is itself tethered to the ER membrane by a poorly described mechanism (Otsu *et al.*, 2006), would thus allow direct presentation of unfolded toxin to the retro-translocon. Oxidized PDI, which is no longer capable of binding and unfolding toxin, is then released from the membrane and replaced by reduced PDI. This binding–release cycle is perpetuated by regeneration of reduced PDI by unknown reductase activity. Clearly, addressing how Ero1α is coupled physically to the retro-translocation machinery, as well as how reduced PDI is regenerated, will elucidate the precise mechanism by which CTA1 is primed for retro-translocation across the ER membrane.

ACKNOWLEDGMENTS

We thank Heather Krueger for critical review of this manuscript. B.T. holds an Investigators in Pathogenesis of Infectious Disease Award from the Burroughs Wellcome Fund.

REFERENCES

Appenzeller-Herzog, C., and Ellgaard, L. (2008). In vivo reduction-oxidation state of protein disulfide isomerase: the two active sites independently occur in the reduced and oxidized forms. Antioxid. Redox Signal. *10*, 55–64.

Bernardi, K. M., Forster, M. L., Lencer, W. I., and Tsai, B. (2008). Derlin-1 facilitates the retro-translocation of cholera toxin. Mol. Biol. Cell *3*, 877–884.

Bernardi, K. M., Williams, J. M., Kikkert, M., van Voorden, S., Wiertz, E. J., Ye, Y., and Tsai, B. (2010). The E3 ubiquitin ligases Hrd1 and gp78 bind to and promote cholera toxin retro-translocation. Mol. Biol. Cell *21*, 140–151.

Bertoli, G., Simmen, T., Anelli, T., Molteni, S. N., Fesce, R., and Sitia, R. (2004). Two conserved cysteine triads in human Ero1alpha cooperate for efficient disulfide bond formation in the endoplasmic reticulum. J. Biol. Chem. *279*, 30047–30052.

Cabibbo, A., Pagani, M., Fabbri, M., Rocchi, M., Farmery, M. R., Bulleid, N. J., and Sitia, R. (2000). ERO1-L, a human protein that favors disulfide bond formation in the endoplasmic reticulum. J. Biol. Chem. *275*, 4827–4833.

Courageot, J., Fenouillet, E., Bastiani, P., and Miquelis, R. (1999). Intracellular degradation of the HIV-1 envelope glycoprotein. Eur. J. Biochem. *260*, 482–489.

Ellgaard, L., and Ruddock, L. W. (2005). The human protein disulphide isomerase family: substrate interactions and functional properties. EMBO Rep. *6*, 28–32.

Forster, M. L., Sivick, K., park, Y. N., Arvan, P., Lencer, W. I., and Tsai, B. (2006). Protein disulfide isomerase-like proteins play opposing roles during retrotranslocation. J. Cell Biol. *173*, 853–859.

Forster, M. L., Mahn, J. J., and Tsai, B. (2009). Generating an unfoldase from thioredoxin-like proteins. J. Biol. Chem. *284*, 13045–13056.

Frand, A. R., and Kaiser, C. A. (1998). The ERO1 gene of yeast is required for oxidation of protein dithiols in the endoplasmic reticulum. Mol. Cell *1*, 161–170.

Frand, A. R., and Kaiser, C. A. (1999). Ero1p oxidizes protein disulfide isomerase in a pathway for disulfide bond formation in the endoplasmic reticulum. Mol. Cell. *4*, 469–477.

Fujinaga, Y., Wolf, A. A., Rodighiero, C., Wheeler, H., Tsai, B., Allen, L., Jobling, M. G., Rapoport, T., Holmes, R. K., and Lencer, W. I. (2003). Gangliosides that associate with lipid rafts mediate transport of cholera and related toxins from the plasma membrane to endoplasmic reticulum. Mol. Biol. Cell *14*, 4783–4793.

Hazes, B., and Read, R. J. (1997). Accumulating evidence suggests that several AB-toxins subvert the endoplasmic reticulum-associated protein degradation pathway to enter target cells. Biochemistry *36*, 11051–11054.

Lencer, W. I., and Tsai, B. (2003). The intracellular voyage of cholera toxin: going retro. Trends Biochem. Sci. *28*, 639–645.

Lilley, B. N., and Ploegh, H. L. (2004). A membrane protein required for dislocation of misfolded proteins from the ER. Nature *429*, 834–840.

Lilley, B. N., and Ploegh, H. L. (2005). Multiprotein complexes that link dislocation, ubiquitination, and extraction of misfolded proteins from the endoplasmic reticulum membrane. Proc. Natl. Acad. Sci. USA *102*, 14296–14301.

Mezghrani, A., Fassio, A., Benham, A., Simmen, T., Braakman, I., and Sitia, R. (2001). Manipulation of oxidative protein folding and PDI redox state in mammalian cells. EMBO J. *20*, 6288–6296.

Molinari, M., Galli, C., Piccaluga, V., Pieren, M., and Paganetti, P. (2002). Sequential assistance of molecular chaperones and transient formation of covalent complexes during protein degradation from the ER. J. Cell Biol. *158*, 247–257.

Oda, Y., Okada, T., Yoshida, H., Kaufman, R. J., Nagata, K., and Mori, K. (2006). Derlin-2 and Derlin-3 are regulated by the mammalian unfolded protein response and are required for ER-associated degradation. J. Cell Biol. *172*, 383–393.

Otsu, M., Bertoli, G., Fagioli, C., Guerini-Rocco, E., Nerini-Molteni, S., Ruffato, E., and Sitia, R. (2006). Dynamic retention of Ero1alpha and Ero1beta in the endoplasmic reticulum by interactions with PDI and ERp44. Antioxid. Redox Signal. *8*, 274–282.

Pagani, M., Fabbri, M., Benedetti, C., Fassio, A., Pilati, S., Bulleid, N. J., Cabibbo, A., and Sitia, R. (2000). Endoplasmic reticulum oxidoreductin 1–1beta (ERO1-Lbeta), a human gene induced in the course of the unfolded protein response. J. Biol. Chem. *275*, 23685–23692.

Pirneskoski, A., Klappa, P., Lobell, M., Williamson, R. A., Byrne, L., Alanen, H. I., Salo, K.E.H., Kivirikko, K. I., Freedman. R. B., and Ruddock, L. W. (2004). Molecular characterization of the principal substrate binding site of the ubiquitous folding catalyst protein disulfide isomerase. J. Biol. Chem. *279*, 10374–10381.

Pollard, M. G., Travers, K. J., and Weissman, J. S. (1998). Ero1p: a novel and ubiquitous protein with an essential role in oxidative protein folding in the endoplasmic reticulum. Mol. Cell *1*, 171–182.

Rodighiero, C., Tsai, B., Rapoport, T. A., and Lencer, W. I. (2002). Role of ubiquitination in retro-translocation of cholera toxin and escape of cytosolic degradation. EMBO Rep. *3*, 1222–1227.

Schulze, A., Standera, S., Buerger, E., Kikkert, M., van Voorden, S., Wiertz, E., Koning, F., Kloetzel, P. M., and Seeger, M. (2005). The ubiquitin-domain protein HERP forms a complex with components of the endoplasmic reticulum associated degradation pathway. J. Mol. Biol. *354*, 1021–1027.

Sears, C. L., and Kaper, J. B. (1996). Enteric bacterial toxins: mechanisms of action and linkage to intestinal secretion. Microbiol. Rev. *60*, 167–215.

Sevier, C. S., and Kaiser, C. A. (2008). Ero1 and redox homeostasis in the endoplasmic reticulum. Biochim. Biophys. Acta *1783*, 549–556.

Spangler, B. D. (1992). Structure and function of cholera toxin and the related *Escherichia coli* heat-labile enterotoxin. Microbiol. Rev. *56*, 622–647.

Tiwari, S., and Weissman, A. M. (2001). Endoplasmic reticulum (ER)-associated degradation of T cell receptor subunits. Involvement of ER-associated ubiquitin-conjugating enzymes (E2s). J. Biol. Chem. *276*, 16193–16200.

Tsai, B., Ye, Y., and Rapoport, T. A. (2002). Retro-translocation of proteins from the endoplasmic reticulum into the cytosol. Nat. Rev. Mol. Cell Biol. *3*, 246–255.

Tsai, B., Rodighiero, C., Lencer, W. I., and Rapoport, T. A. (2001). Protein disulfide isomerase acts as a redox-dependent chaperone to unfold cholera toxin. Cell *104*, 937–948.

Tsai, B., and Rapoport, T. A. (2002). Unfolded cholera toxin is transferred to the ER membrane and released from protein disulfide isomerase upon oxidation by Ero1. J. Cell Biol. *159*, 207–216.

Uemura, A., Oku, M., Mori, K., and Yoshida, H. (2009). Unconventional splicing of XBP1 mRNA occurs in the cytoplasm during the mammalian unfolded protein response. J. Cell Sci. *122*, 2877–2886.

Vembar, S. S., and Brodsky, J. L. (2008). One step at a time: endoplasmic reticulum-associated degradation. Nat. Rev. Mol. Cell Biol. *9*, 944–957.

Wahlman, J., DeMartino, G. N., Skach, W. R., Bulleid, N. J., Brodsky, J. L., and Johnson, A. E. (2007). Real-time fluorescence detection of ERAD substrate retrotranslocation in a mammalian *in vitro* system. Cell *129*, 943–955.

Wainwright, L. J., and Field, M. C. (1997). Quality control of glycosylphosphatidylinositol anchor attachment in mammalian cells: a biochemical study. Biochem. J. *321*, 655–664.

Ye, Y., Shibata, Y., Yun, C., Ron, D., and Rapoport, T. A. (2004). A membrane protein complex mediates retro-translocation from the ER lumen into the cytosol. Nature *429*, 841–847.

Ye, Y., Shibata, Y., Kikkert, M., van Voorden, S., Wiertz, E., and Rapoport, T. A. (2005). Recruitment of the p97ATPase and ubiquitin ligases to the site of retrotranslocation at the endoplasmic reticulum membrane. Proc. Natl. Acad. Sci. USA *102*, 14132–14138.

Young, J., Kane, L. P., Exley, M., and Wileman, T. (1993). Regulation of selective protein degradation in the endoplasmic reticulum by redox potential. J. Biol. Chem. *268*, 19810–19818.

Yu, H., Kaung, G., Kobayashi, S., and Kopito, R. R. (1997). Cytosolic degradation of T-cell receptor alpha chains by the proteasome. J. Biol. Chem. *272*, 20800–20804.

Zhang, H., Peters, K. W., Sun, F., Marino, C. R., Lang, J., Burgoyne, R. D., and Frizzell, R. A. (2002). Cysteine string protein interacts with and modulates the maturation of the cystic fibrosis transmembrane conductance regulator. J. Biol. Chem. *277*, 28948–28958.